



Human Papilloma Virus Circulating Cell-Free DNA Kinetics in Patients with Cervical Cancer Undergoing Definitive Chemoradiation

Aaron Seo¹, Weihong Xiao², Olsi Gjyshi¹, Kyoko Yoshida-Court¹, Peng Wei³, David Swanson³, Tatiana Cisneros Napravnik¹, Adam Grippin¹, Aradhana M. Venkatesan⁴, Megan C. Jacobsen⁵, David T. Fuentes⁵, Erica Lynn¹, Julie Sammour¹, Anuja Jhingran¹, Melissa Joyner¹, Lilie L. Lin¹, Lauren E. Colbert¹, Maura L. Gillison, and Ann H. Klopp¹

ABSTRACT

Purpose: Human papillomavirus (HPV) is a significant cause of cervical cancer. We hypothesized that detecting viral cell-free HPV DNA (cfDNA) before, during, and after chemoradiation (chemoRT) could provide insights into disease extent, clinical staging, and treatment response.

Experimental Design: A total of 66 patients with locally advanced cervical cancer were enrolled between 2017 and 2023, with 49 receiving standard-of-care treatment and 17 participating in a clinical trial combining a therapeutic HPV vaccine (PDS0101; IMMUNOCERV). Plasma was collected at baseline, weeks 1, 3, and 5 of chemoRT, and 3 to 4 months after chemoRT. HPV cfDNA was quantified using droplet digital PCR targeting the HPV E6/E7 oncogenes of 13 high-risk types. MRI was performed at baseline and before brachytherapy.

Results: The median follow-up was 23 months, with recurrence-free survival (RFS) of 78.4% at 2 years. Baseline nodal

disease extent correlated with HPV cfDNA levels. HPV cfDNA levels peaked in week 1 of radiation and decreased through treatment. Patients receiving the PDS0101 vaccine had a higher rate of undetectable HPV type 16 cfDNA compared with those who received standard-of-care therapy. HPV cfDNA clearance correlated with better 2-year RFS (92.9% vs. 30%, log-rank; $P = 0.0067$). The strongest predictor of RFS was HPV cfDNA clearance in follow-up achieving a concordance index score of 0.83, which improved when combined with MRI response (concordance index, 0.88).

Conclusions: HPV cfDNA levels change dynamically during chemoRT. HPV cfDNA levels at follow-up predict RFS, and delivery of therapeutic HPV vaccine with chemoRT was linked to rapid HPV cfDNA decline. Monitoring HPV cfDNA during and after chemoRT may guide tailoring of personalized treatment.

Introduction

Cervical cancer remains a significant health challenge, with a risk of relapse despite aggressive treatment regimens, including chemoradiation (chemoRT) with external beam and brachytherapy (BT; 1–3). Approximately 40% of patients will relapse and 14% will experience grade 3 or higher gastrointestinal, genitourinary, or vaginal toxicity (4, 5). These rates of relapse and toxicity underscore the urgent need for reliable early markers of relapse to enhance clinical decision-making and patient outcomes.

The role of human papillomavirus (HPV) in the pathogenesis of cervical cancer is well-established, positioning HPV-derived biomarkers as potential candidates for monitoring disease dynamics

(6–8). Among these, circulating free DNA (cfDNA), including ctDNA, shows promise in various oncologic settings, reflecting tumor burden and treatment response (9–12). However, the detection capabilities and utility of cfDNA in cervical cancer are less well-documented, particularly as an evolving marker over the course of chemoRT, highlighting a gap in our current understanding of how cfDNA clearance can be utilized to inform treatment response. Furthermore, the relative predictive power of cfDNA as compared with radiographic response, which is routinely incorporated into cervical cancer treatment, has not been evaluated (13–17).

We proposed that HPV cfDNA can serve as a biomarker for predicting and monitoring treatment response in cervical cancer and may be complementary with imaging-based responses on MRI and 2[18F]fluoro-2-deoxy-D-glucose (¹⁸F FDG) PET/CT. To evaluate this, we measured HPV cfDNA clearance (a measure of ctDNA in HPV-associated cervical cancers) in patients with cervical cancer receiving definitive chemoRT. Our study incorporates patients treated with either standard-of-care (SOC) chemoRT or with an immunotherapy–chemoRT combination from a recently completed trial involving PDS0101, a novel therapeutic vaccine targeting HPV-related cancers. As PDS0101 represents a new avenue in the immunotherapy landscape, we also present a descriptive comparison of HPV cfDNA profiles in patients treated with PDS0101 versus SOC.

Materials and Methods

Study design: SOC tissue-banking studies

Study patients were enrolled in two longitudinal tissue-banking studies (SWAB2014-0543 and CoACH2019-1059). Informed written

¹Department of Radiation Oncology, University of Texas MD Anderson Cancer Center, Houston, Texas. ²Thoracic/Head and Neck Medical Oncology Department, University of Texas MD Anderson Cancer Center, Houston, Texas. ³Department of Biostatistics, University of Texas MD Anderson Cancer Center, Houston, Texas. ⁴Division of Diagnostic Imaging, Department of Abdominal Imaging, University of Texas MD Anderson Cancer Center, Houston, Texas. ⁵Department of Imaging Physics, University of Texas MD Anderson Cancer Center, Houston, Texas.

Corresponding Author: Ann H. Klopp, Department of Radiation Oncology, University of Texas MD Anderson Cancer Center, 1515 Holcombe Boulevard, Houston, TX 77030. E-mail: aklopp@mdanderson.org

Clin Cancer Res 2025;31:697–706

doi: 10.1158/1078-0432.CCR-24-2343

©2024 American Association for Cancer Research

Translational Relevance

Despite aggressive definitive treatment including chemoradiation (chemoRT) with external beam radiation and brachytherapy, about 40% of patients with cervical cancer will ultimately relapse, and about half will experience chronic toxicity. Given the high rates of relapse and toxicity, early markers of relapse are urgently needed to improve clinical decision-making and patient outcomes. These results demonstrate that detectable human papillomavirus plasma DNA after chemoRT is associated with worse recurrence-free survival, and combining this potential biomarker with imaging metrics of response can better predict patient outcomes. Detecting human papillomavirus plasma DNA shortly during and after completing chemoRT may be useful tools in the future to inform both treatment escalation as well as de-escalation.

consent was obtained from each subject or each subject's guardian. Inclusion criteria were patients ≥ 18 years of age with HPV-positive locally advanced cervical cancer International Federation of Gynecology and Obstetrics (FIGO, 2018 stages IB3-IVA), who are candidates eligible for curative concurrent chemoradiotherapy. Exclusion criteria include those patients younger than 18 years of age with operable tumors, those with coexisting medical conditions that would preclude chemotherapy or radiotherapy, pregnant patients, those unwilling or unable to comply with study and/or follow-up procedures, and those with contraindications to either contrast-enhanced CT or MRI. Treatment for women with locally advanced cervical cancer was concurrent weekly cisplatin (40 mg/m^2) chemotherapy (up to five cycles) with external beam radiotherapy (EBRT) and BT delivered in < 8 weeks (18). Patients received 1.8 to 2 Gy/fractions (fx) of EBRT to a total dose of 45 to 50 Gy using intensity-modulated radiation therapy with CT planning followed by BT (either high dose rate or pulsed dose rate BT) and nodal boost if appropriate. The planning target volume was created by placing five to seven margins around the nodal clinical target volume and central pelvic internal target volume (volume covering the gross tumor, and at-risk vagina and cervix taking into account tumor and organ interfractional motion). Patients without nodal involvement or with involvement limited to the pelvic nodes were treated with radiation to the pelvis. The upper field border extended to the level of the aortic bifurcation. Patients with positive common iliac nodes also received radiation to the lower periaortic nodes, while those with positive periaortic nodes were treated along the entire periaortic lymph node chain. Daily image guidance was performed with kV or cone-beam CT (CBCT) for position verification. Nodal boosts to pathologically enlarged lymph nodes were delivered with integrated boosts (2 Gy/ per fx) and sequential boosts as needed to bring the total dose to nodes (including external beam primary fields, boost fields, and any BT contribution) to equivalent dose in 2 Gy fx of 60 to 66 Gy. Image-guided BT was delivered within 7 days of completion of primary EBRT with either high dose rate (five insertions) or pulsed dose rate BT (two insertions). Tandem and cylinder, ring, ovoid, or hybrid applicators were used as needed to achieve optimal applicator placement. The target dose for the high-risk clinical target volume was greater than 87 Gy

while limiting the D2cc (dose to maximally exposed 2 cm^3) bladder dose to less than 80 Gy, the rectal dose to < 70 Gy, and the sigmoid dose to < 70 Gy. Please refer to Supplementary Table S1 for additional details.

Study design: IMMUNOCERV trial protocol

The IMMUNOCERV trial was a single-arm, phase 2 study (NCT04580771; IMMUNOCERV2019-1260) designed to test the hypothesis that PDS0101, a novel, subcutaneously administered HPV-specific vaccine containing peptide pools encoding E6/E7 antigens, would be safe and effective in combination with SOC chemoRT for locally advanced HPV-related cervical cancer. Patients received PDS0101 at days -10 , 7 , 28 , and 49 (± 5 days) in relation to the start of SOC chemoRT. Key eligibility criteria included newly diagnosed, biopsy-proven locally advanced squamous cell carcinoma of the cervix (tumor $\geq 5 \text{ cm}$ and/or nodal disease), > 18 years of age, and Eastern Cooperative Oncology Group ≤ 2 . Please refer to Supplementary Table S1 for additional details.

Blood collection

Peripheral blood samples were collected in Cell-Free DNA BCT tubes (Streck). After centrifuging at $1,600 \times g$ for 10 minutes at room temperature, plasma was carefully transferred to microcentrifuge tubes and centrifuged at $16,000 \times g$ for 10 minutes to remove any blood cells. Then, plasma was stored in 1-mL aliquots in screw cap tubes at -80°C . Please refer to Supplementary Table S2 for additional details.

cfDNA isolation

cfDNA was purified with 1 mL of plasma using QIAamp Circulating Nucleic Acid Kit (QIAGEN) with vacuum processing following the manufacturer's instructions. Briefly, plasma samples were thawed and digested with proteinase K and lysis buffer containing $1 \mu\text{g}$ carry RNA per sample to complete the release of nucleic acids from bound proteins, lipids, and vesicles. Lysates were then absorbed onto a QIAamp Mini column by vacuum pressure. After washing the column, circulating nucleic acids were eluted in $60 \mu\text{L}$ of AVE buffer and stored at -20°C until analysis.

cfHPV droplet digital PCR analysis

To detect high-risk single copies of HPV16 or HPV18, 31, 33, 35, 39, 45, 51, 52, 56, 58, 59, and 68 DNA, a dual-target droplet digital PCR (ddPCR) method was developed using the sequence of their HPV E6 or E7 oncogenes (19). The specific primers and probes for seven dual-target PCR assays were designed, including HPV sequence variance and phylogenetic variables. The probes were differentially fluorescence-tagged for the simultaneous detection and quantification of both types. The human endogenous retrovirus group 3 (*ERV3*) gene was used as human DNA quality control. Seven dual-target ddPCR assays are pairs of HPV16-*ERV3*, HPV18-HPV33, HPV33-HPV35, HPV31-HPV58, HPV52-HPV59, HPV39-HPV51, and HPV56-HPV68. The primers and probes for each HPV type were designed to avoid cross-reaction among 13 high-risk HPV types. HPV ddPCR assay was performed on the QX200 Droplet Digital PCR System (Bio-Rad). Each reaction assay contained $5 \mu\text{L}$ of $4\times$ ddPCR supermix for probe (no dUTP), 0.9 nmol/L of respective primers, 0.25 nmol/L of respective probes, 4 units of restriction enzyme BamH1, and $13 \mu\text{L}$ of elute in a final volume of $20 \mu\text{L}$. The mix was vortexed and loaded into a Bio-Rad carriage to generate droplets, $40 \mu\text{L}$ of droplets were transferred into a PCR plate and sealed with pierceable foil. PCR was performed as one cycle of 95°C for 10 minutes, 40 cycles of 94°C

for 30 seconds and 57.1°C for 1 minute, and one cycle of 95°C for 10 minutes; and the step ramp rate was 2°C per second. The amplified droplets were detected in a Bio-Rad reader. Data were analyzed to determine HPV types and copy numbers using QuantaSoft software. Measures of ≥ 16 copies/mL, which were considered quantifiable, were previously described and classified as detectable for the analysis (19). In brief, to determine the limit of quantitation (LoQ), the lowest concentration at which the analyte can be accurately detected, HPV16 fragment DNA was serially diluted and spiked into 2 mL of plasma from patients without cancer or HPV infection. From each concentration, cfDNA was extracted and tested using the HPV16/ERV3 ddPCR reaction in triplicate. This analysis revealed that 16 copies/mL plasma was the LoQ for HPV16, indicating the lowest concentration at which the virus could be reliably detected. This methodology was similarly applied to the other 12 high-risk HPV types. The LoQ for plasma cfDNA established at 16 copies per 1 mL plasma for all tested high-risk HPV types. “Undetectable” and “detectable” cfDNA were designated “cleared” and “uncleared” statuses, respectively.

Statistical analysis

The χ^2 test was used to compare the distributions of HPV types between primary tumor swabs and peripheral blood. cfDNA levels below 16 were adjusted to the quantifiable threshold of 16 copies/mL. Then, all values underwent \log_{10} transformation for further analysis. The Fisher exact test and Wilcoxon rank-sum test were used to compare sociodemographic and clinical factors across cohort types. The Shapiro–Wilk test was used for normality testing of continuous variables. The Kruskal–Wallis test was used to associate cfDNA levels at different timepoints with sociodemographic and clinical factors. The Dunn test was used to conduct *post hoc* pairwise comparisons to identify specific groups with differences identified by the Kruskal–Wallis test.

Recurrence-free survival (RFS) was defined as the time from histologic diagnosis of cervical cancer to the time of the first recurrence. The Kaplan–Meier method was used to estimate RFS and compared with the log-rank test. Factors associated with RFS were evaluated with the Cox proportional hazards model. Univariable analysis included the following factors: cohort designation, age at diagnosis, ethnicity, body mass index, smoking status, FIGO 2018 stage, highest involved lymph node at diagnosis, number of cisplatin cycles, baseline MRI gross tumor volume (GTV), MRI GTV during week 5 of treatment, and GTV regression [defined as: $1 - (\text{GTV}_{\text{week 5 of treatment}}/\text{GTV}_{\text{baseline}})$]. Optimal GTV regression was defined as GTV regression ≥ 0.90 , as previously described; (ref. 13). HPV cfDNA levels were measured before treatment, during week 1 of treatment, during week 3 of treatment, during week 5 of treatment, and in follow-up, 3 to 4 months after completion of therapy. Given the limited follow-up sample size and events, multivariable analysis for RFS was restricted to two variables: follow-up HPV cfDNA level (continuous) and number of cisplatin cycles.

Concordance indices were calculated to quantify the predictive accuracy of predictive variables. The C-index is analogous to the area under the receiver-operating characteristic curve for binary outcomes but modified to account for censoring in time-to-event outcomes. Similar to the area under the receiver-operating characteristic curve, a c-index of 1.0 indicates perfect classification, whereas a value of 0.5 suggests random guessing. All statistical analyses were performed using R version 4.2.1.

Ethics statement

The clinical studies were conducted according to the guidelines of the Declaration of Helsinki and approved by the institutional review

board of The University of Texas MD Anderson Cancer Center (SWAB2014-0543, CoACH2019-1059, and IMMUNOCERV2019-1260). Informed consent was obtained from all study participants.

Data availability

The deidentified data that support the findings of this study will be available on reasonable request. The data are not publicly available due to protected health information that could compromise the privacy of research participants.

Results

Cohort demographic and clinical characteristics

Between 2017 and 2023, 66 patients with locally advanced cervical cancer were enrolled on this longitudinal study (49 SOC patients and 17 PDS0101 patients). All patients were treated with definitive chemoRT with BT boost, and all patients received concurrent cisplatin. Patients on the PDS0101 study received the HPV-directed vaccine before, during, and after chemoRT. For the overall cohort, the median follow-up was 23 months, with a 2-year RFS of 78.4% [95% confidence interval (CI), 67.5%–91.0%].

Sociodemographic factors were balanced between the two cohorts (Table 1). Clinical factors such as FIGO 2018 stage, baseline and mid-treatment GTV MRI volume measurements, GTV treatment response on MRI, number of cisplatin cycles, baseline and follow-up maximum standardized uptake values (SUV) on ^{18}F FDG PET/CT were balanced between the two cohorts (Table 2). The pattern of lymph node involvement differed between the PDS0101 and SOC cohorts. Lymph node involvement was more common in the PDS0101 cohort compared with SOC (100% vs. 73%). However, PDS0101 patients predominantly had pelvic lymph nodes as the highest clinically involved level, while SOC patients were more likely to have involvement of the common iliac and para-aortic lymph nodes ($P = 0.009$; Table 2).

HPV tumor and plasma genotyping

HPV typing of primary tumor swabs showed that 69% (43/62) of tumors were HPV type 16 or 18, 16% (10/62) were other high-risk HPV types, and 15% (9/62) were negative (Fig. 1A). The distributions of HPV types in cfDNA at any available timepoint compared with tumor swabs was similar (χ^2 test; $P = 0.55$); 62% (41/66) of cfDNA HPV types were 16 or 18, 11% (7/66) were other high-risk HPV types, and 27% (18/66) were negative (Fig. 1B). Patients who did not have the same HPV genotype could be attributed to being nonshedders, discordant, or not detected in the primary site. Twelve patients with primary tumor swabs who demonstrated high-risk HPV types were negative in plasma cfDNA at all available timepoints. This may relate to biological differences in tumor biology, including lower rates of cell turnover or decreased tumor vascularization. Four patients had discordant positive HPV types in primary tumor swabs and plasma (one patient with type 31 in tumor and type 18 in plasma; one patient with type 16 in tumor and type 45 in plasma; and two patients with type 18 in tumor and type 16 in plasma). These discordant cases may be attributable to heterogeneity in tumor with multiple HPV types that may have variable propensity to release tumor DNA into circulation. Of the nine patients with no HPV type detected in the primary tumor with swab testing, four patients had a detectable high-risk HPV type in plasma (two patients with HPV type 16 and two patients with HPV type 18). These cases may reflect failure to sample HPV type in the primary tumor.

Table 1. Sociodemographic characteristics.

| Characteristic | Overall, N = 66 ^a | PDS, N = 17 ^a | SOC, N = 49 ^a | P value ^b |
|---|------------------------------|--------------------------|--------------------------|----------------------|
| Age (years) | 44.8 (11.7) | 44.1 (14.2) | 45.0 (10.9) | 0.5 |
| Body mass index (kg/m ²) | 28.9 (5.9) | 26.7 (3.7) | 29.7 (6.4) | 0.12 |
| Ethnicity | | | | 0.2 |
| Declined to answer | 2 (3.0%) | 1 (5.9%) | 1 (2.0%) | |
| Hispanic or Latino | 18 (27%) | 2 (12%) | 16 (33%) | |
| Not Hispanic or Latino | 46 (70%) | 14 (82%) | 32 (65%) | |
| Race | | | | 0.2 |
| Asian | 1 (1.5%) | 1 (5.9%) | 0 (0%) | |
| Black or African American | 6 (9.1%) | 2 (12%) | 4 (8.2%) | |
| Native Hawaiian or other Pacific Islander | 1 (1.5%) | 1 (5.9%) | 0 (0%) | |
| Other | 9 (14%) | 1 (5.9%) | 8 (16%) | |
| Unknown or declined to answer | 4 (6.1%) | 1 (5.9%) | 3 (6.1%) | |
| White | 45 (68%) | 11 (65%) | 34 (69%) | |
| Smoking status | | | | 0.8 |
| Current | 8 (12%) | 2 (12%) | 6 (12%) | |
| Former | 19 (29%) | 6 (35%) | 13 (27%) | |
| Never | 39 (59%) | 9 (53%) | 30 (61%) | |

^aMean (SD); n (%).^bWilcoxon rank-sum test; Fisher exact test.**Baseline HPV cfDNA levels and clinical characteristics**

With the 50 available baseline HPV cfDNA levels, the median value was 27.9 copies/mL (range, 16.0–2.06 × 10⁵). The differences in baseline HPV cfDNA levels across FIGO 2018 stage were not statistically significant (*P* = 0.11; **Fig. 1C**), although stage IV patients had the highest median value (1.87 × 10⁴ copies/mL)

compared with stages I, II, and III (16.0, 27.6, and 28.2, respectively). Baseline HPV cfDNA levels were significantly different across different categories of the highest echelon involved lymph node level at time of diagnosis (*P* = 0.02; **Fig. 1D**). Patients with para-aortic involvement had the highest median baseline HPV cfDNA (1.36 × 10⁴ copies/mL), which on *post hoc* pairwise comparisons was

Table 2. Clinical characteristics.

| Characteristic | Overall, N = 66 ^a | PDS, N = 17 ^a | SOC, N = 49 ^a | P value ^b |
|--|------------------------------|--------------------------|--------------------------|----------------------|
| FIGO 2018 stage | | | | 0.6 |
| I | 4 (6.1%) | 1 (5.9%) | 3 (6.1%) | |
| II | 12 (18%) | 2 (12%) | 10 (20%) | |
| III | 46 (70%) | 12 (71%) | 34 (69%) | |
| IV | 4 (6.1%) | 2 (12%) | 2 (4.1%) | |
| Highest node/involved node | | | | 0.009 |
| Common iliac | 12 (18%) | 2 (12%) | 10 (20%) | |
| Not involved | 13 (20%) | 0 (0%) | 13 (27%) | |
| Para-aortic | 12 (18%) | 2 (12%) | 10 (20%) | |
| Pelvic | 29 (44%) | 13 (76%) | 16 (33%) | |
| Baseline GTV volume on MRI (cm ³) | 71 (78) | 68 (59) | 72 (84) | 0.5 |
| Pre-BT GTV volume on MRI (cm ³) | 14 (28) | 13 (20) | 14 (30) | 0.2 |
| Unknown | 6 | 0 | 6 | |
| GTV treatment response on MRI (continuous) | 0.90 (0.76, 0.97) | 0.86 (0.77, 0.92) | 0.90 (0.76, 1.00) | 0.2 |
| Unknown | 7 | 0 | 7 | |
| GTV treatment response on MRI (threshold: 90%) | | | | 0.11 |
| Optimal | 27 (46%) | 5 (29%) | 22 (52%) | |
| Suboptimal | 32 (54%) | 12 (71%) | 20 (48%) | |
| Unknown | 7 | 0 | 7 | |
| Cisplatin cycles received | | | | 0.6 |
| 1–3 | 4 (6.1%) | 2 (12%) | 2 (4.1%) | |
| 4+ | 58 (88%) | 14 (82%) | 44 (90%) | |
| Other | 4 (6.1%) | 1 (5.9%) | 3 (6.1%) | |
| Baseline maximum SUV on PET-CT | 19 (13) | 19 (7) | 19 (15) | 0.4 |
| Unknown | 4 | 1 | 3 | |
| 3–4 months f/u maximum SUV on PET-CT | 3.47 (1.66) | 2.96 (1.21) | 3.69 (1.79) | 0.063 |
| Unknown | 9 | 0 | 9 | |

^an (%); mean (SD); median (IQR).^bFisher's exact test; Wilcoxon rank-sum test; Pearson's χ^2 test.

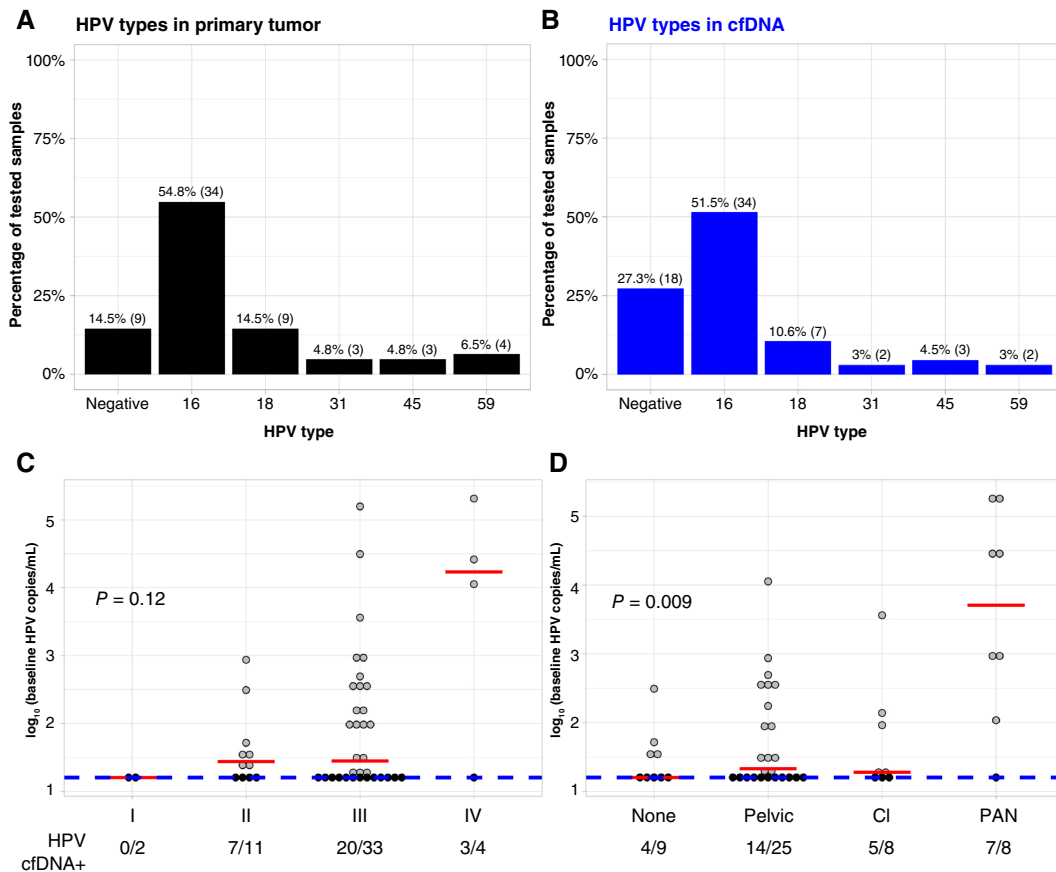


Figure 1.

HPV types and baseline characteristics. **A**, HPV types from primary tumor swabs. **B**, HPV types from cfDNA for patients from whom both tumor swab and cfDNA HPV typing was performed. **C**, Pretreatment cfDNA levels by FIGO 2018 stage. **D**, Pretreatment cfDNA levels by the highest involved lymph node at diagnosis. PAN, para-aortic lymph nodes. Gray dots, detectable cfDNA levels; black dots, below the limit of detection; red line, the median value; and blue dotted line, the limit of detection. Kruskal-Wallis rank sum *P* values are reported.

significantly different compared with common iliac involvement (median, 19.0 copies/mL; *P* = 0.0076), pelvic lymph node involvement (median, 21.4 copies/mL; *P* = 0.0012), and having no involved lymph nodes (median, 16.0 copies/mL; *P* = 0.0011; **Fig. 1D**). There was no significant difference in *post hoc* pairwise comparisons of baseline HPV cfDNA levels in other levels of lymph node involvement. Baseline cfDNA levels were not significantly correlated to baseline GTV on MRI (*P* = 0.24) or baseline maximum SUV on ¹⁸F FDG PET/CT (*P* = 0.57).

HPV cfDNA kinetics during and after definitive chemoRT

During treatment, the median HPV cfDNA level peaked during week 1 (median, 42.3 copies/mL; range, 16.0–3.13 × 10⁴) and subsequently decreased through treatment (week 3: median, 16.0 copies/mL; range, 16.0–1.25 × 10⁵; week 5: median, 16.0 copies/mL; range, 16.0–3,780) and in 3- to 4-month follow-up (median, 16.0 copies/mL; range, 16.0–789; **Fig. 2A**). Of the 66 patients with at least one timepoint measurement available, six patients (9.1%) never had cfDNA detected (**Fig. 2A**; Supplementary Fig. S1). Of the 45 patients with at least three timepoint measurements, 26.7% of patients had peak cfDNA levels at baseline, and 40% had peak cfDNA levels during week 1 of treatment (**Fig. 2B**). Clearance of cfDNA levels progressively increased during treatment, starting with

HPV cfDNA undetected at baseline in 40% of patients, HPV cfDNA undetected during week 1 of treatment in 35.6% of patients, HPV cfDNA undetected during week 3 of treatment in 60% of patients, and HPV cfDNA undetected during week 5 of treatment in 81.0% (Supplementary Fig. S2A). At the 3- to 4-month follow-up, 76.2% of patients had undetectable HPV cfDNA.

Earlier HPV type 16 cfDNA clearance in patients receiving PDS0101 therapeutic vaccine compared with SOC

Because the PDS0101 vaccine is derived from HPV type 16 peptides, we hypothesized that patients who received the PDS0101 vaccine would have a greater HPV type 16 cfDNA clearance rate compared with SOC. The PDS0101 vaccine cohort had a greater percentage of patients with undetectable HPV type 16 cfDNA at each ascertainable timepoint (**Fig. 2C**). Furthermore, patients who received the PDS0101 vaccine also experienced greater HPV cfDNA clearance at each timepoint when considering all HPV types. (Supplementary Fig. S2B).

Detected HPV cfDNA at 3 to 4 months of follow-up associated with reduced RFS

Given that HPV cfDNA clearance increases throughout treatment and plateaus near the end of treatment, we hypothesized that

Downloaded from <http://aacrjournals.org/clinccancerres/article-pdf/31/4/697/3541512/ccr-24-2343.pdf> by guest on 08 April 2025

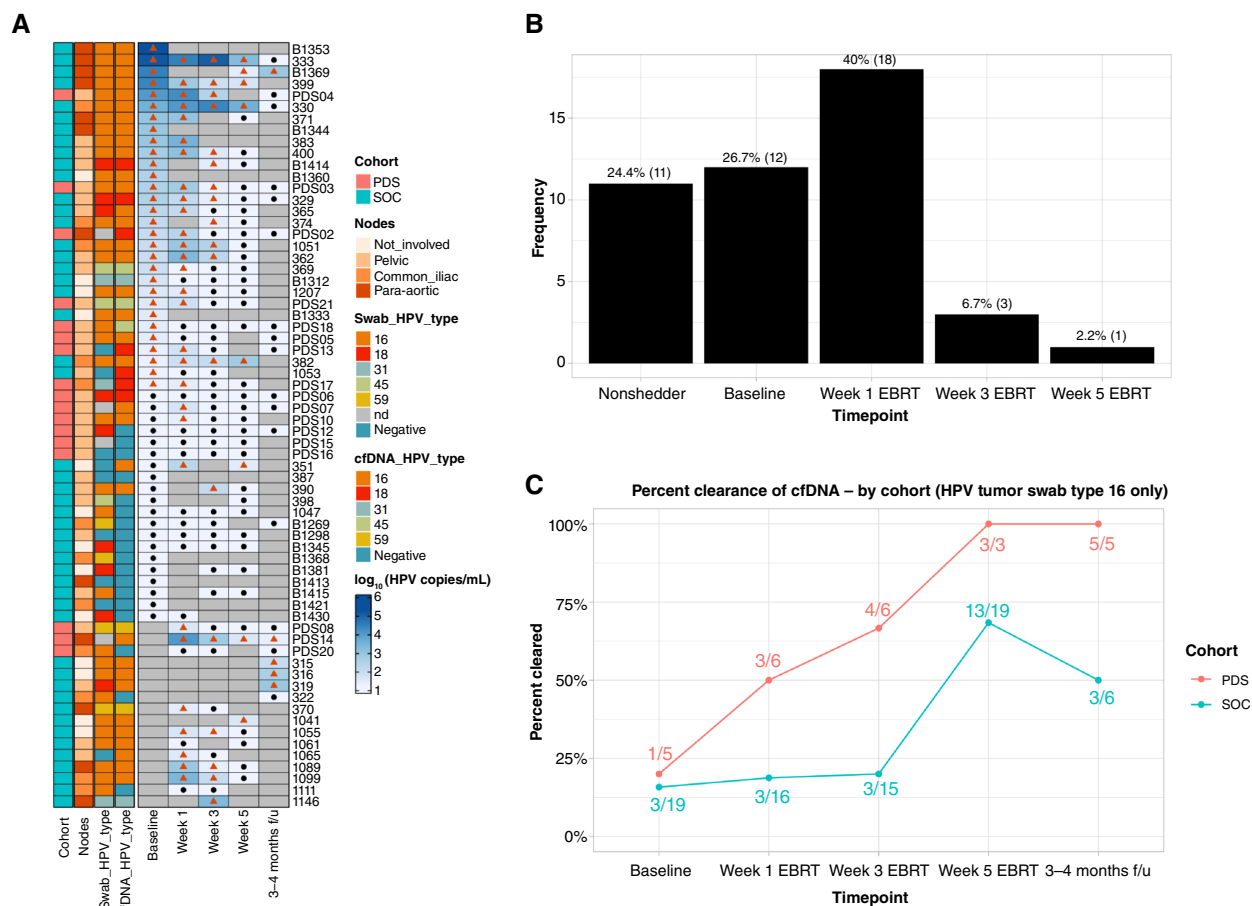


Figure 2.

HPV cfDNA kinetics. **A**, Heatmap of HPV cfDNA levels from before, during, and after definitive chemoRT. Gray shade, not tested; black dot, level below the limit of detection; and red triangle, above the limit of detection. **B**, Counts of the timepoints at which peak cfDNA levels were measured in patients with at least three timepoint measurements. **C**, Percentage of patients with HPV cfDNA type 16 clearance (below the limit of detection) by timepoint. nd, not determined.

the presence of HPV cfDNA near the end of treatment and at 3- to 4-month follow-up would be associated with inferior survival outcomes. HPV cfDNA clearance at baseline or during treatment (weeks 1, 3, and 5) was not significantly associated with RFS (**Fig. 3A–C**). Detectable vs. undetectable HPV cfDNA at 3- to 4-month follow-up were associated with worse RFS [2-year RFS estimate 30.0% (95% CI, 6.31%–100%) vs. 92.9% (95% CI, 80.3%–100%); log-rank $P = 0.0067$; **Fig. 3D**]. Furthermore, this association pattern was also true for patients with detectable HPV cfDNA before follow-up and eventually had clearance at follow-up (Supplementary Fig. S4). On univariable Cox regression analysis, HPV cfDNA levels at 3- to 4-month follow-up was the only significant variable associated with RFS [HR, 7.21 (95% CI, 1.79–28.96; $P = 0.005$; **Table 3**)].

Predictive accuracy of HPV cfDNA levels, MRI, and ^{18}F FDG PET/CT responses on RFS

To compare the performance of HPV cfDNA levels and various imaging modalities to predict RFS and to determine whether these variables were complementary or synergistic, we measured the concordance indices for HPV cfDNA levels at 3- to 4-month follow-up, GTV volumetric reduction from before treatment to pre-BT

(MRI response), and PET/CT FDG avidity at 3- to 4-month follow-up (PET/CT). C-indices for HPV cfDNA levels at 3- to 4-month follow-up, MRI response, and ^{18}F FDG PET/CT (maximum SUV at follow-up) were 0.83 ± 0.12 , 0.60 ± 0.09 , and 0.49 ± 0.11 , respectively. The c-index for HPV cfDNA levels at 3- to 4-month follow-up and MRI response combined was 0.88 ± 0.1 . Multivariable Cox regression analysis showed an increased hazard ratio for HPV cfDNA levels at 3- to 4-month follow-up when adjusted for MRI [HR, 9.54 (95% CI, 0.920–99.0; $P = 0.0588$; Supplementary Table S2)].

Discussion

In this prospective collection study from a large tertiary cancer center, we describe HPV cfDNA kinetics before, during, and after definitive chemoRT in patients with locally advanced cervical cancer, including patients receiving the PDS0101 therapeutic vaccine derived from HPV E6 and E7 peptides. In the pooled analysis, quantifiable HPV cfDNA at 3- to 4-month follow-up was associated with inferior RFS, whereas HPV cfDNA levels at other timepoints before and during chemoRT were not associated with RFS. HPV types in primary tumors and plasma were largely concordant, with some of the discordances stemming from undetected HPV types in

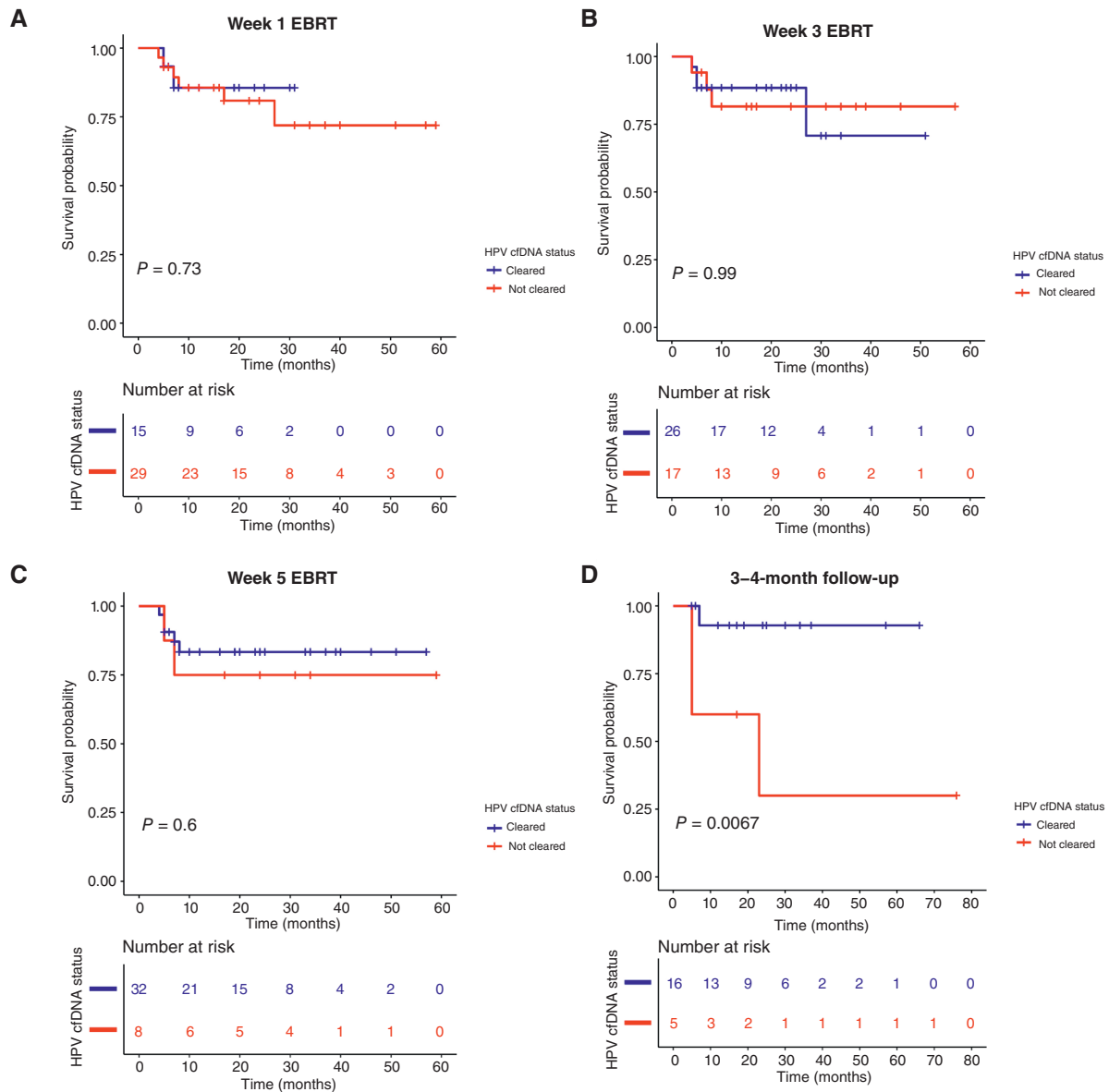


Figure 3.

Kaplan-Meier curves for RFS stratified by detectable vs. undetectable HPV cfDNA (A) during week 1 EBRT, (B) during week 3 EBRT, (C) during week 5 EBRT, and (D) at 3- to 4-month follow-up. The log-rank test P values are reported.

primary tumors with detection in plasma. One potential explanation for this discordant pattern is a false-negative primary tumor swab from insufficient sampling, in which plasma HPV cfDNA could assist in accurately characterizing the HPV association of a patient's cervical cancer, which can have important prognostic implications as HPV-negative cervical cancers are associated with worse outcomes than those that are HPV-associated (20–25).

Baseline HPV cfDNA levels were most strongly associated with the highest involved lymph node at the time of diagnosis, with the highest levels in patients with para-aortic lymph node involvement. Of note, primary tumor size was not associated with baseline HPV cfDNA level, suggesting that ctDNA is most reflective of regional spread rather than local disease burden.

We show that HPV cfDNA levels generally rise and peak early during chemoRT, suggesting tumor cellular death and genomic shedding early in treatment. HPV cfDNA levels subsequently nadir at the completion of chemoRT. The slight increase in percent HPV cfDNA clearance at 3- to 4-month follow-up suggests that HPV cfDNA clearance can continue to occur after completing definitive chemoRT.

Of note, on exploratory subanalysis, the patients who received PDS0101, a therapeutic vaccine derived from HPV type 16 E6 and E7 peptides, experienced greater and earlier clearance of HPV type 16 cfDNA compared with patients receiving SOC treatment. This difference could reflect vaccine efficacy with respect to immune system recognition of the E6 and E7 viral

Table 3. Univariable Cox regression analysis for RFS.

| | All | HR (univariable) |
|--|-------------|-------------------------------------|
| Cohort | | |
| SOC | 49 (74.2) | — |
| PDS | 17 (25.8) | 0.55 (0.12–2.54; <i>P</i> = 0.447) |
| FIGO 2018 stage | | |
| I | 4 (6.1) | — |
| II | 12 (18.2) | 0.32 (0.02–5.22; <i>P</i> = 0.427) |
| III | 46 (69.7) | 0.73 (0.09–5.80; <i>P</i> = 0.763) |
| IV | 4 (6.1) | 1.41 (0.09–22.79; <i>P</i> = 0.809) |
| Highest involved lymph node | | |
| Not involved | 13 (19.7) | — |
| Pelvic | 29 (43.9) | 2.45 (0.29–20.34; <i>P</i> = 0.408) |
| Common iliac | 12 (18.2) | 1.00 (0.06–15.99; <i>P</i> = 0.999) |
| Para-aortic | 12 (18.2) | 4.44 (0.49–39.80; <i>P</i> = 0.183) |
| Cisplatin cycles | | |
| 1–3 | 4 (6.1) | — |
| 4+ | 58 (87.9) | 0.21 (0.04–1.01; <i>P</i> = 0.052) |
| Other | 4 (6.1) | 0.00 (0.00–Inf; <i>P</i> = 0.998) |
| Baseline MRI GTV volume (cm ³) | | |
| Mean (SD) | 71.2 (77.6) | 1.00 (1.00–1.01; <i>P</i> = 0.165) |
| Week 5 MRI GTV volume (cm ³) | | |
| Mean (SD) | 13.6 (27.5) | 1.01 (0.99–1.03; <i>P</i> = 0.370) |
| MRI GTV treatment response | | |
| Mean (SD) | 0.8 (0.2) | 0.24 (0.01–11.38; <i>P</i> = 0.468) |
| Maximum SUV on PET-CT: baseline | | |
| Mean (SD) | 19.4 (13.2) | 0.96 (0.87–1.05; <i>P</i> = 0.357) |
| Maximum SUV on PET-CT: follow-up | | |
| Mean (SD) | 3.5 (1.7) | 1.06 (0.72–1.56; <i>P</i> = 0.760) |
| Baseline ctDNA (log ₁₀ -transformed) | | |
| Mean (SD) | 2.0 (1.1) | 1.71 (0.98–2.98; <i>P</i> = 0.060) |
| Week 1 EBRT ctDNA (log ₁₀ -transformed) | | |
| Mean (SD) | 2.0 (1.0) | 1.03 (0.51–2.10; <i>P</i> = 0.933) |
| Week 3 EBRT ctDNA (log ₁₀ -transformed) | | |
| Mean (SD) | 1.6 (0.8) | 1.65 (0.96–2.85; <i>P</i> = 0.070) |
| Week 5 EBRT ctDNA (log ₁₀ -transformed) | | |
| Mean (SD) | 1.4 (0.5) | 1.37 (0.48–3.94; <i>P</i> = 0.553) |
| Follow-up ctDNA (log ₁₀ -transformed) | | |
| Mean (SD) | 1.5 (0.6) | 7.21 (1.79–28.96; <i>P</i> = 0.005) |

peptides. Additional detailed immunoprofiling from patient samples will help clarify the effects of the therapeutic vaccine. Although patients receiving PDS0101 were included in this report, the study was not statistically powered for survival outcomes comparisons between cohorts, which will be the focus of additional studies.

A select number of studies have explored serial measurements of HPV cfDNA levels (26–33). The largest prospective study to date assessing ctDNA levels in patients with cervical cancer receiving definitive chemoRT [Han and colleagues (34)] evaluated 70 total patients at three timepoints: end of chemoRT, 4 to 6 weeks after chemoRT, and 3 months after chemoRT. Our study provides unique insights into early changes in HPV cfDNA during radiation treatment. We observed an increase in HPV cfDNA for patients during the first week of radiation. This rapid increase in tumor DNA in circulation may reflect intracellular contents being released upon cell death. Although we did not detect a relationship between week 1 cfDNA and outcome, these early changes suggest that rapid cfDNA kinetic changes may be a potential early-response biomarker, meriting further evaluation with additional timepoints and patients.

Han and colleagues found that detectable HPV ctDNA at all three timepoints was significantly associated with inferior 2-year progression-free survival (PFS) with a median lead time to recurrence of 5.9 months. In contrast, our study did not find a significant difference in RFS with quantifiable HPV cfDNA in the last week of external beam chemoRT, suggesting that HPV cfDNA status at the end of total chemoRT but not midtreatment may be prognostic. Han and colleagues utilized both ddPCR and a next-generation sequencing approach and found that both approaches had similar results. This finding lends credence to our use of ddPCR and also has encouraging implications for testing access worldwide, as ddPCR is, in general, less costly than next-generation sequencing technologies (35). Furthermore, the performance of HPV cfDNA levels at 3-month follow-up to predict RFS/PFS based on the c-index was equivalent in our study and Han and colleagues (c-index = 0.72; ref. 34). Although Han and colleagues did not include routine ¹⁸F FDG PET/CT follow-up as part of their study, our study showed that combining HPV cfDNA levels and ¹⁸F FDG PET/CT follow-up yields a higher c-index (0.92), suggesting a multimodal surveillance approach may be more effective at detecting early recurrence. Unlike Han and colleagues, our study evaluated the combined use of on-treatment MRI response and cfDNA response and suggested an additive benefit of these two biomarkers. Larger prospective cohorts will help validate these results.

Recently, concurrent and adjuvant immunotherapy has been demonstrated to improve PFS for patients with locally advanced cervical cancer (36). The benefits of this intensified treatment, however, come at the cost of significantly higher toxicity (75% vs. 69% grade 3 or higher adverse events) as well as significant time under treatment and costs, as patients received 15 cycles of pembrolizumab every 6 weeks (37, 38). Our study suggests that HPV cfDNA levels may help tailor treatment by identifying a high-risk population during radiation treatment who may benefit from treatment escalation with adjuvant immunotherapy therapy (38). Furthermore, cfHPV DNA analysis may also help to identify patients with an excellent early response who may benefit from radiation dose de-escalation to avoid toxicities associated with high-dose radiation treatment.

The strengths of this study include robust imaging correlates, including primary tumor HPV swab typing, cfDNA monitoring early in radiation treatment, midtreatment MRI and a 3- to 4-month follow-up ¹⁸F FDG PET/CT scan in the majority of patients, use of modern radiation therapy techniques, use of Streck tubes for optimal plasma preservation, multiple intratreatment timepoints, and the first report of ctDNA kinetics in patients receiving the PDS0101 therapeutic vaccine. Limitations of the study include limited follow-up sample collection and no additional timepoints between the end of chemoRT and 3- to 4-month follow-up.

In conclusion, we found that quantifiable HPV cfDNA at 3- to 4-month follow-up was associated with inferior RFS. The PDS0101 therapeutic vaccine was associated with greater and earlier clearance of HPV type 16 cfDNA. Additional follow-up and studies are needed to assess for differences in survival outcomes with PDS0101 and to ascertain the clinical utility of HPV cfDNA testing during and after chemoRT to guide treatment de-escalation as well as escalation with adjuvant systemic therapy.

Authors' Disclosures

K. Yoshida-Court reports other support from PDS Biotechnology Corporation during the conduct of the study. A. Grippin reports a pending patent for his work related to cancer vaccines. A.M. Venkatesan reports grants from Siemens

Healthineers outside the submitted work. E. Lynn reports grants and nonfinancial support from PDS Biotechnology Corporation during the conduct of the study. L.L. Lin reports grants from the NCI, AstraZeneca, Pfizer, and Varian Medical Systems and other support from Trevarx Biomedical, Inc., outside the submitted work. M.L. Gillison reports other support from LLX Solutions, Eisai Medical Research, Sensei Biotherapeutics, Inc., BioNTech SE, EMD Serono, Inc., Kura Oncology, Inc., Gilead Sciences, Inc., Debiopharm, Seagen Inc. (formerly Seattle Genetics), OncLive (owned by Intellisphere, LLC), Istari Oncology Inc., iTeos Therapeutics, Coherus BioSciences, Caladrius Biosciences, Inc., Exelixis, Inc., Shattuck Labs, Surface Oncology, Inc., Suzhou Liangyihi Network Technology, Bristol Myers Squibb, Merus N.V., Boxer Capital, LLC, AbbVie, Pfizer, Brightly Network, Guidepoint Global Consulting, Bicara Therapeutics, Aptitude Health, Axiom Healthcare, Adaptimmune, Ispen Biopharmaceuticals, the American Society of Clinical Oncology, NRG-HN008, and the KURRENT-HN trial; other support from SKYSCRAPER trial Roche, Merck (University of Cincinnati), InVax, and Genentech, Inc., outside the submitted work; in addition, M.L. Gillison has a patent for PCT/US2022/023911 pending to the Board of Regents, The University of Texas System. A.H. Klopp reports grants from PDS Biotechnology Corporation during the conduct of the study. No disclosures were reported by the other authors.

Authors' Contributions

A. Seo: Conceptualization, data curation, software, formal analysis, validation, investigation, visualization, methodology, writing—original draft, writing—review and editing. **W. Xiao:** Data curation, software, formal analysis, investigation, methodology, writing—original draft, writing—review and editing. **O. Gjyshi:** Conceptualization, data curation, software, formal analysis, methodology, writing—review and editing. **K. Yoshida-Court:** Conceptualization, data curation, software, formal analysis, validation, writing—original draft, writing—review and editing. **P. Wei:** Formal analysis, methodology, writing—original draft, writing—review and editing. **D. Swanson:** Investigation, methodology, writing—original draft, writing—review and editing. **T. Cisneros Napravnik:** Conceptualization, resources, data

curation, writing—original draft, writing—review and editing. **A. Grippin:** Data curation, writing—review and editing. **A.M. Venkatesan:** Conceptualization, resources, data curation, investigation, visualization, writing—review and editing. **M.C. Jacobsen:** Data curation, validation, writing—review and editing. **D.T. Fuentes:** Data curation, validation, writing—review and editing. **E. Lynn:** Resources, data curation, writing—review and editing. **J. Sammouri:** Data curation. **A. Jhingran:** Resources, writing—review and editing. **M. Joyner:** Resources, writing—review and editing. **L.L. Lin:** Resources, writing—review and editing. **L.E. Colbert:** Resources, data curation, investigation, writing—review and editing. **M.L. Gillison:** Conceptualization, resources, data curation, supervision, investigation, methodology, writing—original draft, writing—review and editing. **A.H. Klopp:** Conceptualization, resources, data curation, formal analysis, supervision, investigation, visualization, methodology, writing—original draft, writing—review and editing.

Acknowledgments

We would like to thank Van Morris and Jia Sun for helpful discussions. We thank PDS Biotechnology Corporation for funding and provision of PDS0101 (Versamune HPV) for the IMMUNOCERV clinical trial. This work was supported in part by the generous philanthropic contributions to The University of Texas MD Anderson Cancer Center Moon Shots Program and the HPV-related Cancers Moon Shot and also supported by the NIH/NCI under award number P30CA016672.

Note

Supplementary data for this article are available at Clinical Cancer Research Online (<http://clincancerres.aacrjournals.org/>).

Received July 22, 2024; revised October 16, 2024; accepted December 12, 2024; published first December 16, 2024.

References

- Arbyn M, Weiderpass E, Bruni L, de Sanjosé S, Saraiya M, Ferlay J, et al. Estimates of incidence and mortality of cervical cancer in 2018: a worldwide analysis. *Lancet Glob Health* 2020;8:e191–203.
- Siegel RL, Miller KD, Jemal A. Cancer statistics, 2020. *CA Cancer J Clin* 2020; 70:7–30.
- Rose PG, Bundy BN, Watkins EB, Thigpen JT, Deppe G, Maiman MA, et al. Concurrent cisplatin-based radiotherapy and chemotherapy for locally advanced cervical cancer. *N Engl J Med* 1999;340:1144–53.
- Eifel PJ, Winter K, Morris M, Levenback C, Grigsby PW, Cooper J, et al. Pelvic irradiation with concurrent chemotherapy versus pelvic and para-aortic irradiation for high-risk cervical cancer: an update of radiation therapy oncology group trial (RTOG) 90-01. *J Clin Oncol* 2004;22:872–80.
- Vittrup AS, Kirchheiner K, Pötter R, Fokdal LU, Jensen NBK, Spampinato S, et al. Overall severe morbidity after chemo-radiation therapy and magnetic resonance imaging-guided adaptive brachytherapy in locally advanced cervical cancer: results from the EMBRACE-I study. *Int J Radiat Oncol Biol Phys* 2023; 116:807–24.
- Dürst M, Gissmann L, Ikenberg H, zur Hausen H. A papillomavirus DNA from a cervical carcinoma and its prevalence in cancer biopsy samples from different geographic regions. *Proc Natl Acad Sci U S A* 1983;80:3812–5.
- Gissmann L, Wolnik L, Ikenberg H, Koldovsky U, Schnürch HG, zur Hausen H. Human papillomavirus types 6 and 11 DNA sequences in genital and laryngeal papillomas and in some cervical cancers. *Proc Natl Acad Sci U S A* 1983;80:560–3.
- Crum CP, Ikenberg H, Richart RM, Gissman L. Human papillomavirus type 16 and early cervical neoplasia. *N Engl J Med* 1984;310:880–3.
- Karimi A, Jafari-Koshki T, Zehabi M, Kargar F, Gheit T. Predictive impact of human papillomavirus circulating tumor DNA in treatment response monitoring of HPV-associated cancers; a meta-analysis on recurrent event endpoints. *Cancer Med* 2023;12:17592–602.
- Tie J, Cohen JD, Lahouel K, Lo SN, Wang Y, Kosmider S, et al. Circulating tumor DNA analysis guiding adjuvant therapy in stage II colon cancer. *N Engl J Med* 2022;386:2261–72.
- Pellini B, Chaudhuri AA. Circulating tumor DNA minimal residual disease detection of non-small-cell lung cancer treated with curative intent. *J Clin Oncol* 2022;40:567–75.
- Galati L, Combes J-D, Le Calvez-Kelm F, McKay-Chopin S, Forey N, Ratel M, et al. Detection of circulating HPV16 DNA as a biomarker for cervical cancer by a bead-based HPV genotyping assay. *Microbiol Spectr* 2022;10:e0148021.
- Schernberg A, Bockel S, Annde P, Fumagalli I, Escande A, Mignot F, et al. Tumor shrinkage during chemoradiation in locally advanced cervical cancer patients: prognostic significance, and impact for image-guided adaptive brachytherapy. *Int J Radiat Oncol Biol Phys* 2018;102:362–72.
- Schernberg A, Kumar T, Achkar S, Espenel S, Bockel S, Majer M, et al. Incorporating magnetic resonance imaging (MRI) based radiation therapy response prediction into clinical practice for locally advanced cervical cancer patients. *Semin Radiat Oncol* 2020;30:291–9.
- Kidd EA, El Naqa I, Siegel BA, Dehdashti F, Grigsby PW. FDG-PET-based prognostic nomograms for locally advanced cervical cancer. *Gynecol Oncol* 2012;127:136–40.
- Kidd EA, Siegel BA, Dehdashti F, Rader JS, Mutch DG, Powell MA, et al. Lymph node staging by positron emission tomography in cervical cancer: relationship to prognosis. *J Clin Oncol* 2010;28:2108–13.
- Kidd EA, Siegel BA, Dehdashti F, Grigsby PW. The standardized uptake value for F-18 fluorodeoxyglucose is a sensitive predictive biomarker for cervical cancer treatment response and survival. *Cancer* 2007;110:1738–44.
- Chemoradiotherapy for Cervical Cancer Meta-Analysis Collaboration. Reducing uncertainties about the effects of chemoradiotherapy for cervical cancer: a systematic review and meta-analysis of individual patient data from 18 randomized trials. *J Clin Oncol* 2008;26:5802–12.
- Wotman MT, Xiao WX, Du RR, Jiang B, Liu S, Gillison ML. Development and validation of an assay to quantify plasma cell-free human papillomavirus DNA for 13 high-risk types that cause 98% of HPV-positive cancers. *J Clin Oncol* 2024;42(suppl 16):6065.
- Tjalma WAA, Trinh XB, Rosenlund M, Makar AP, Kridelka F, Rosillon D, et al. A cross-sectional, multicentre, epidemiological study on human papillomavirus (HPV) type distribution in adult women diagnosed with invasive cervical cancer in Belgium. *Facts Views Vis Obgyn* 2015;7:101–8.
- Barreto CL, Martins DB, de Lima Filho JL, Magalhães V. Detection of human Papillomavirus in biopsies of patients with cervical cancer, and its association with prognosis. *Arch Gynecol Obstet* 2013;288:643–8.

22. Romero-Pastrana F. Detection and typing of human papilloma virus by multiplex PCR with type-specific primers. *ISRN Microbiol* 2012;2012:186915.
23. Baay MF, Tjalma WA, Weyler J, Pattyn GG, Lambrechts HA, Goovaerts G, et al. Prevalence of human papillomavirus in elderly women with cervical cancer. *Gynecol Obstet Invest* 2001;52:248–51.
24. Higgins GD, Davy M, Roder D, Uzelin DM, Phillips GE, Burrell CJ. Increased age and mortality associated with cervical carcinomas negative for human papillomavirus RNA. *Lancet* 1991;338:910–3.
25. Riou G, Favre M, Jeannot D, Bourhis J, Le Doussal V, Orth G. Association between poor prognosis in early-stage invasive cervical carcinomas and non-detection of HPV DNA. *Lancet* 1990;335:1171–4.
26. Widschwendter A, Blassnig A, Wiedemair A, Müller-Holzner E, Müller HM, Marth C. Human papillomavirus DNA in sera of cervical cancer patients as tumor marker. *Cancer Lett* 2003;202:231–9.
27. Yang HJ, Liu VWS, Tsang PCK, Yip AMW, Tam KF, Wong LC, et al. Quantification of human papillomavirus DNA in the plasma of patients with cervical cancer. *Int J Gynecol Cancer* 2004;14:903–10.
28. Campitelli M, Jeannot E, Peter M, Lappartient E, Saada S, de la Rochefordière A, et al. Human papillomavirus mutational insertion: specific marker of circulating tumor DNA in cervical cancer patients. *PLoS One* 2012;7:e43393.
29. Han K, Leung E, Barbera L, Barnes E, Croke J, Di Grappa MA, et al. Circulating human papillomavirus DNA as a biomarker of response in patients with locally advanced cervical cancer treated with definitive chemoradiation. *JCO Precision Oncol* 2018;2:1–8.
30. Cabel L, Bonneau C, Bernard-Tessier A, Héquet D, Tran-Perennou C, Bataillon G, et al. HPV ctDNA detection of high-risk HPV types during chemoradiotherapy for locally advanced cervical cancer. *ESMO Open* 2021;6:100154.
31. Jeannot E, Latouche A, Bonneau C, Calmèjane M-A, Beaufort C, Ruigrok-Ritstier K, et al. Circulating HPV DNA as a marker for early detection of relapse in patients with cervical cancer. *Clin Cancer Res* 2021;27:5869–77.
32. Lalondrelle S, Lee J, Cutts RJ, Garcia Murillas I, Matthews N, Turner N, et al. Predicting response to radical chemoradiotherapy with circulating HPV DNA (cHPV-DNA) in locally advanced uterine cervix cancer. *Cancers (Basel)* 2023; 15:1387.
33. Mittelstadt S, Kelemen O, Admard J, Gschwind A, Koch A, Wörz S, et al. Detection of circulating cell-free HPV DNA of 13 HPV types for patients with cervical cancer as potential biomarker to monitor therapy response and to detect relapse. *Br J Cancer* 2023;128:2097–103.
34. Han K, Zou J, Zhao Z, Baskurt Z, Zheng Y, Barnes E, et al. Clinical validation of human papilloma virus circulating tumor DNA for early detection of residual disease after chemoradiation in cervical cancer. *J Clin Oncol* 2024;42: 431–40.
35. Mattox AK, D'Souza G, Khan Z, Allen H, Henson S, Seiwert TY, et al. Comparison of next generation sequencing, droplet digital PCR, and quantitative real-time PCR for the earlier detection and quantification of HPV in HPV-positive oropharyngeal cancer. *Oral Oncol* 2022;128: 105805.
36. Lorusso D, Xiang Y, Hasegawa K, Scambia G, Leiva M, Ramos-Elias P, et al. Pembrolizumab or placebo with chemoradiotherapy followed by pembrolizumab or placebo for newly diagnosed, high-risk, locally advanced cervical cancer (ENGOT-cx11/GOG-3047/KEYNOTE-A18): a randomised, double-blind, phase 3 clinical trial. *Lancet* 2024;403:1341–50.
37. Lindegaard JC, Petric P, Tan L-T, Hoskin P, Schmid MP, Jürgenliemk-Schulz I, et al. Are we making progress in curing advanced cervical cancer-again? *Int J Gynecol Cancer* 2024;34:1940–5.
38. Mileschkin LR, Moore KN, Barnes EH, GebSKI V, Narayan K, King MT, et al. Adjuvant chemotherapy following chemoradiotherapy as primary treatment for locally advanced cervical cancer versus chemoradiotherapy alone (OUT-BACK): an international, open-label, randomised, phase 3 trial. *Lancet Oncol* 2023;24:468–82.